Intelligent Maneuvering Decision System for Computer Generated Forces Using Predictive Fuzzy Inference System

Tsung-Ying Sun, *Member*, *IEEE*
Department of Electrical Engineering, National Dong Hwa University, Hualien, Taiwan, R.O.C.
Email: sunty@mail.ndhu.edu.tw

Shang-Jeng Tsai, *Student Member*, *IEEE* and Chih-Li Huo
Department of Electrical Engineering, National Dong Hwa University, Hualien, Taiwan, R.O.C.
Email: d9123001@em91.ndhu.edu.tw and m9623045@em96.ndhu.edu.tw

***Abstract*—The purpose of this paper is to develop an intelligent maneuvering decision system (IMDS) for computer generated forces (CGF). The proposed CGF can take actions similar to a human pilot to gain an advantageous status over the enemy target using the IMDS. The IMDS will produce the best control command from the control alternatives for the CGF in an air combat environment. In this paper, a predictive fuzzy inference system (PFIS) is proposed as the IMDS for CGF, which incorporates and mimics human thinking capability and the maximum capacity of CGF. Before PFIS executes the fuzzy inference system (FIS) process, it will generate the control alternatives from CGF's decision space, and allow CGF to predict its future posture. This study assumes that CGF can accurately predict an enemy target's future position, and then PFIS applies the predicted data to generate the best control command. In this paper, the proposed algorithm is verified with two types of fighter flying data that are used as the enemy target's flying trajectories. The simulation and discussion of the proposed algorithm shows that PFIS will enable CGF to obtain the best status in an air combat environment and the performance of the proposed algorithm will be affected by the CGF's prediction ability for enemy target.**

***Index Terms*—intelligent maneuvering decision system (IMDS), computer generated forces (CGF), predictive fuzzy inference system (PFIS)**

I. Introduction

In today's world, the development of the computer generated forces (CGF) built-in flight simulator is important for training pilots' maneuvering skill in an air combat environment. In most flight simulator, the restricted functions offer the virtual aircrafts simple dynamics which can provide only unrealistic flight training. The most important goal of developing CGF is to produce genuine, life-like air battle simulations, in order to improve pilots' capabilities and survivability in an air combat environment. In order to assess and make decisions according to the battle environments immediately, CGF must act similar to the mind of a pilot. It does not only reduce the cost of pilot training, but also increases the usability of flight simulators. Thus, the development of an intelligent decision making mechanism is critical in CGF [1]-[6].

Intelligent maneuvering decision system (IMDS) is similar to a general evader-pursuer maneuvering automation problem between two highly interactive objects' dynamic systems. The majority of approaches to the problems of maneuvering automation rely heavily on optimization techniques using differential game theory [7]-[12].

For the purpose of keeping these above mentioned problems mathematically tractable and solvable, some limitations are necessary. These limitations include: pursuer and evader moving with simple dynamics, and saddle-point values of the cost function to each problems must also exist. These limitations deviates the solution from what is realistic in combat situations of experienced pilots.

The objective of developing CGF is to obtain advantageous flight status over the enemy target in simulated air combat environment. Examples such as keeping the enemy in range of its shooting envelop, allowing the CGF to enter the best shooting distance, and attacking the enemy while maintaining an optimal speed and a safe height. In this paper, a predictive fuzzy inference system (PFIS) is proposed as the IMDS for CGF. The PFIS will produce the best control command from the control alternatives for CGF in an air combat environment. This paper assumes the CGF could accurately predict the future posture of an enemy target. The control alternatives are composed of CGF's decision space. The best control command would be generated by PFIS reasoning procedure. In this paper, the proposed algorithm is verified with two types of fighter flying data used as the enemy target's flying trajectory. The simulation and discussion of the proposed algorithm

Tsung-Ying Sun as corresponding author to provide phone: +886-3-8634078; fax: +886-3-8634060; e-mail: sunty@mail.ndhu.edu.tw

© 2008 ACADEMY PUBLISHER

shows that PFIS will enable CGF to obtain the best status in an air combat environment and the performance of the proposed algorithm will be affected by the CGF's prediction ability for enemy target.

The paper is organized as follows: Section I is the introduction, Section II presents CGF flight dynamic equations. Section III describes the structure of PFIS. Section IV exhibits the simulation results. Section V and Section VI are the discussion and the conclusion respectively.

II. CGF Flight Dynamic Equations

The purpose of developing the IMDS for CGF is to allow the CGF to simulate human pilots' combat behaviors to produce the best control command in an air combat environment. The proposed IMDS for CGF in this paper is based on the fuzzy inference system (FIS). The architecture of IMDS is shown as Fig. 1, the predicted trajectory information of an enemy target fed into IMDS for reasoning the best control command for the flight model of CGF. Due to the simulation, the dynamic equation of CGF controls the virtual flight with maximum capacity.

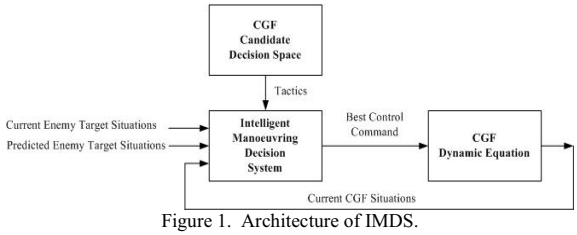

Figure 1. Architecture of IMDS.

There are seven different tactics, maximum G-force left and right turn, maximum acceleration and deceleration, maximum G-force upward and downward flight, and continued stable flight, shown in Fig. 2 [13]. In our study, these seven kinds of flying strategies are executed at maximum capacities in CGF to obtain advantageous status in air combat.

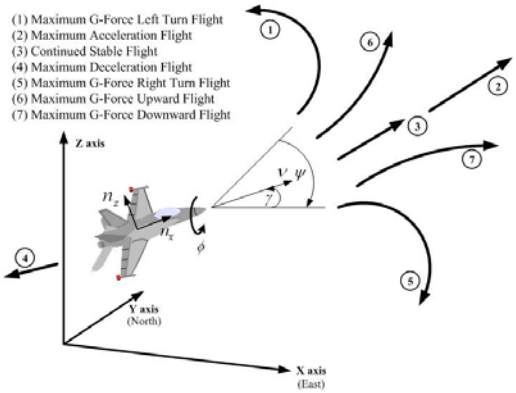

Figure 2. Seven kinds of CGF's tactics

The three-dimensional dynamic behavior of CGF are described in (1), (2) and (3), where x, y and z are CGF's positions in the inertia coordinate system, with units in meters. The value of γ presents the path angle between velocity direction of V and the horizontal plane with units in radians. The value of Ψ is the heading angle between the projection of V and the Y-axis (northward direction) with units in radians. Velocity in x, y and z direction can be obtained from (1) to (3) with units in meters per second.

$$\dot{x} = V\cos\gamma\sin\Psi \tag{1}$$

$$\dot{y} = V\cos\gamma\cos\Psi \tag{2}$$

$$\dot{z} = V\sin\gamma \tag{3}$$

The values of first order differential of V, γ and Ψ are denoted as $\dot{V}$, $\dot{\gamma}$ and $\dot{\Psi}$ respectively, as shown in (4), (5) and (6), where n_x, n_z and ϕ are three control variables of CGF. The "g" stands for the acceleration of gravity and its value and unit is 9.8 (meters per second squared). The first control variable n_x represents the load factor along the direction of V which can be transformed into the thrust force with g's units. The second control variable n_z is the load factor shown as Fig. 2 which can be transformed into the pitch force, its units are also in g's. ϕ is the rolling angle and it can be transformed into the rolling force, and it is the third control variable, its units are in radians.

$$\dot{V} = g(n_x - \sin\gamma) \tag{4}$$

$$\dot{\gamma} = \frac{g}{V}(n_z\cos\phi - \cos\gamma) \tag{5}$$

$$\dot{\Psi} = \frac{gn_z\sin\phi}{V\cos\gamma} \tag{6}$$

The three commands a pilot offers to control flight are denoted as n_{xcom}, n_{zcom} and ϕ_{com}, their units are in g, g, and radians respectively. Due to the existence of inertia, the values of n_x, n_z and ϕ could not coincide with n_{xcom}, n_{zcom} and ϕ_{com} immediately. Therefore, the dynamic delay models are utilized from (7) to (9), where τ_x and τ_z are time constants of n_x and n_z respectively. As the value of τ_x and τ_z increases, the delay time from command n_{xcom} and n_{zcom} to actual response n_x and n_z increases. The values of ω_n and ξ denote natural frequency and damping ratio respectively.

$$n_x = \frac{1}{1+\tau_x s}\times n_{xcom} \tag{7}$$

$$n_z = \frac{1}{1+\tau_z s}\times n_{zcom} \tag{8}$$

$$\phi = \frac{\omega_n^{\,2}}{s^2 + 2\omega_n\xi s + \omega_n^{\,2}}\times\phi_{com} \tag{9}$$

III. The Structure Of IMDS

The purpose of developing IMDS is to give CGF an advantageous flight status over an enemy target such as keeping the enemy target in front of its shooting envelop; or entering the best shooting distance, attacking speed, and height in a safe region at the same time. Based on the posture prediction of the enemy target, IMDS will generate the best control command from the control alternatives via PFIS to drive CGF to its best posture. The structure of IMDS is shown as Fig. 3. The candidate

© 2008 ACADEMY PUBLISHER

decision space of CGF in Fig. 2 uses Table I with maximum capacity for control commands n_{xcom}, n_{zcom} and ϕ_{com} in the seven predefined tactics.

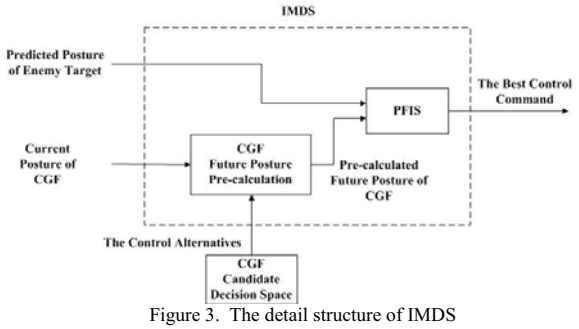

Figure 3. The detail structure of IMDS

TABLE I
THE SEVEN KINDS OF TACTICS FOR CGF'S MAXIMUM CAPACITY

Control command	Tactics Number						
	1	2	3	4	5	6	7
n_{xcom} (g)	0	3	0	-3	0	0	0
n_{zcom} (g)	9	0	0	0	9	9	-9
ϕ_{com} (radian)	$-\pi/2$	0	0	0	$\pi/2$	0	0

The PFIS is composed of fuzzy knowledge base (FKB) and fuzzy inference engine (FIE). The FKB describes the domain knowledge. Through FIE, PFIS will obtain the best control command. The details of PFIS process are described below.

A. Fuzzy Knowledge Base

In an air combat environment, advanced fighters can judge the advantages and disadvantages over an enemy target according to four conditions such as aspect, relative distance, velocity, and height [13]. Defined here as four linguistic variables, μ_A (aspect), μ_R (relative distance), μ_V (velocity), and μ_H (height), by membership functions. The grade values of these membership functions are real numbers between 0 and 1. The closer the value of membership grade is to 1, the more advantageous it is to the CGF for these membership functions. With proper membership functions the model can assess and deliver the most advantageous action. The membership functions of the four linguistic variables are described below. Assuming that the CGF's current situation includes three-dimensional positions x_c, y_c, z_c, velocity V_c, path angle γ_c and heading angle Ψ_c. Assuming also that the enemy target's current situation includes three-dimensional positions x_t, y_t, z_t, velocity V_t, path angle γ_t and heading angle Ψ_t.

1) **Aspect Membership Function**

In an air battle situation, one of the important goals for CGF is to keep the enemy in front of its shooting aspect. The aspect membership function is defined in (10), and is depicted as Fig. 4(a), where θ_c is defined as Fig. 4(b) and denotes the angle between $\vec{R}$ and $\vec{V}_c$. In Fig. 4(b), $\vec{R}$ represents the distance vector from the enemy to CGF, and $\vec{V}_c$ as the velocity vector of CGF. The formulas of $\vec{R}$ and $\vec{V}_c$ are represented in (11). The formula of θ_c is represented in (12), where $\vec{R}^t$ represents the transpose of $\vec{R}$. The closer the membership grade of μ_A is to 1, the closer the enemy target is to CGF's shooting aspect.

$$\mu_A(\theta_c) = \frac{\theta_c}{\pi},\ 0 \le \theta_c \le \pi \tag{10}$$

$$\vec{R} = \begin{bmatrix} x_c - x_t \\ y_c - y_t \\ z_c - z_t \end{bmatrix},\ \vec{V}_c = \begin{bmatrix} V_c \times \cos(\gamma_c) \times \sin(\Psi_c) \\ V_c \times \cos(\gamma_c) \times \cos(\Psi_c) \\ V_c \times \sin(\gamma_c) \end{bmatrix} \tag{11}$$

$$\theta_c = \cos^{-1}\left(\frac{\vec{R}^t \times \vec{V}_c}{\left\|\vec{R}\right\| \times \left\|\vec{V}_c\right\|} \right) \tag{12}$$

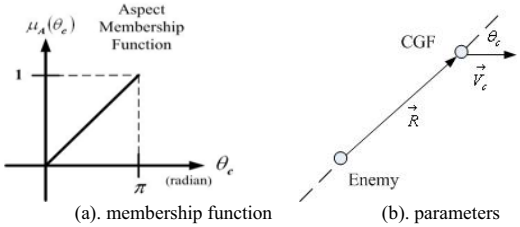

(a). membership function (b). parameters

Figure 4. Aspect membership function

2) **Relative Distance Membership Function**

In air combat, CGF must notice the distance between itself and the enemy. If the distance isn't far enough, CGF may collide with the enemy target. If the distance isn't close enough, the enemy may not be in CGF's effective shooting range. Relative distance membership function is defined in (13), and is depicted as Fig. 5, where R presents the distance between CGF and the enemy, and is represented in (14), R_m is the best shooting distance of CGF, σ is the standard deviation. The closer the membership grade of μ_R is to 1, the better the CGF's attacking distance is to the enemy.

$$\mu_R(R) = \exp\left(-\frac{(R - R_m)^2}{2\sigma^2} \right) \tag{13}$$

$$\vec{R} = \begin{bmatrix} x_c - x_t \\ y_c - y_t \\ z_c - z_t \end{bmatrix},\ R = \left\|\vec{R}\right\| \tag{14}$$

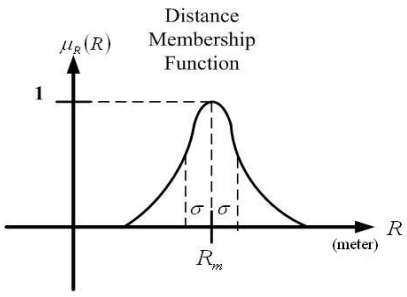

Figure 5. Distance membership function

© 2008 ACADEMY PUBLISHER

3) **Velocity Membership Function**

In an air combat environment, CGF must adjust its velocity according to the relative distance between itself and the enemy target. When their relative distance is too far apart, CGF must increase its velocity in order to approach the enemy target quickly. When the relative distance is close to the best shooting distance, CGF must decrease its velocity for the purpose of tracing and aiming. The velocity membership function is defined as (15) and is depicted in Fig. 6, where V_c represents the velocity of CGF. The best attack velocity of CGF, V_o, is defined in (16), where V_t is the velocity of the enemy target, and $V_{\max}$ is the maximum limited velocity of CGF. The value of V_o is the relationship between R and R_m, where R denotes the distance between CGF and the enemy target, which is represented as in (14), and R_m is CGF's best shooting distance. The closer the membership grade of μ_V is to 1, the more advantageous CGF's velocity is with respect to enemy target.

$$\mu_V(V_c) = \frac{V_c}{V_o}\exp\left(\frac{-2|V_c - V_o|}{V_o}\right) \quad (15)$$

$$V_o = \begin{cases} V_t + (V_{\max} - V_t)\left(1 - \exp\left(\frac{R_m - R}{R_m}\right)\right) & , R > R_m \\ V_t & , R \le R_m \end{cases} \quad (16)$$

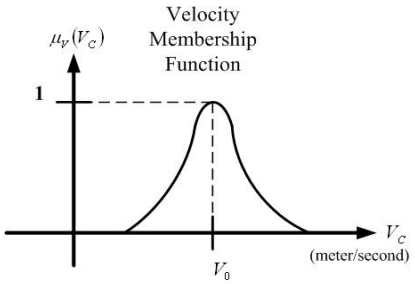

Figure 6. Velocity membership function

4) **Height Membership Function**

When CGF is in an air combat situation, a safe height must be kept to avoid striking a mountain or a building. The height membership function is defined in (17) and is depicted in Fig. 7, where z and h_o denote CGF's height and the minimum limitation of CGF's height, respectively. If z is larger than h_o, CGF is in a safer region; otherwise, it is in a more dangerous region.

$$\mu_H(z) = \begin{cases} \frac{z}{h_o}\exp\left(-2\frac{h_o - z}{h_o}\right), & z \le h_o \\ 1, & z > h_o \end{cases} \quad (17)$$

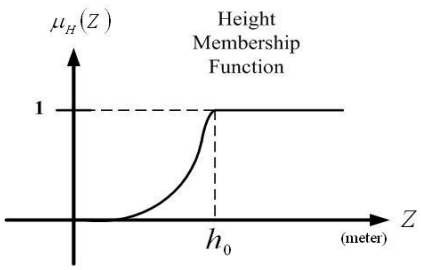

Figure 7. Height membership function

B. Fuzzification Interface

Before PFIS executes fuzzification interface process, it must generate control alternatives composed of CGF's decision space. The CGF can calculate its future posture in advance according to the control alternatives, in addition to an enemy target's future posture. The control alternatives, represented as C_i, are shown in (18). C_i is i-th tactic number of strategy commands in Table I. In (18), T and kT represent sample period and k-th sample period respectively.

$$C_i(kT) = \left[n_{xcom}(kT), n_{zcom}(kT), \phi_{com}(kT)\right]_i,\ i \in \{1,2,...,7\} \quad (18)$$

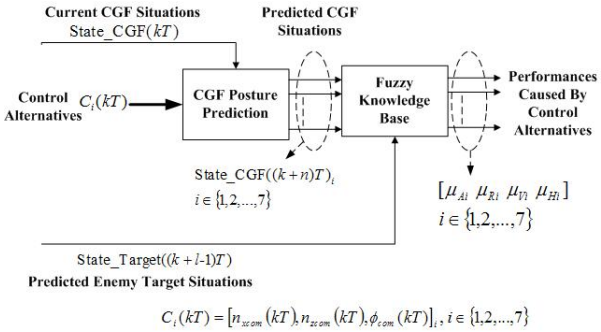

Figure 8. Performances caused by the control alternatives

PFIS will evaluate the performance of control alternatives using four membership functions in the FKB. The current situations of CGF, and the predicted situations of CGF and the enemy target are represented as State_CGF(kT), State_CGF($(k+n)T$) and State_Taget($k+l$-1)T) respectively in Fig. 8, where i, n, l, T, kT , ($k+n$)T and ($k+l$-1)T are the tactic number in Table I, the time delay parameter of CGF's flight dynamic equations, predicted step number, sample period, the k-th, ($k+n$)-th and ($k+l$-1)-th sample period.

1) **Current Situations of CGF**

State_CGF(kT) includes current CGF's three-dimensional position, velocity, flight path angle, and heading angle. These are represented as $x_c(kT)$, $y_c(kT)$, $z_c(kT)$, $V_c(kT)$, $\gamma_c(kT)$ and $\Psi_c(kT)$ respectively.

2) **Predicted Situations of CGF**

CGF can predict the situation of its ($k+n$)-th sample period with the control alternatives represented in (18). The ($k+n$)-th sample period of CGF's situation is represented as State_CGF($(k+n)T$)..

3) **Predicted Situations of Enemy Target**

It is assumed the CGF can predict the enemy target's ($k+l$-1)-th sample period situations, represented as State_Taget($k+l$-1)T). Then the four membership function values with State_CGF($(k+n)T$) and State_Taget($k+l$-1)T) are calculated in the FKB. These membership values are represented as $[\mu_{Ai}\ \mu_{Ri}\ \mu_{Vi}\ \mu_{Hi}]$, where $i \in \{1,2,...,7\}$. These membership values can be regarded as the performance caused by the control alternatives.

© 2008 ACADEMY PUBLISHER

C. Fuzzy Inference Engine using IF-THEN rules

In this paper, PFIS uses fuzzy IF-THEN rules to decide which strategy it should take. The rules are described as (19), where $i \in \{1,2,...,7\}$.

IF

u is $C_i \rightarrow \mu_{Ai}$ is Good and μ_{Ri} is Good and μ_{Vi} is Good and μ_{Hi} is Good (19)

THEN u is C_i

In (19), Good in the linguistic variable means that its membership value is closer to 1. The input u represents the three control command values of control alternatives. Then the min-max principle is applied for fuzzy reasoning operation as Fig. 9.

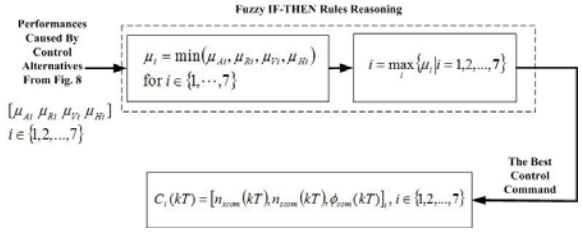

Figure 9. Fuzzy inference engine using IF-THEN rules for reasoning

D. PFIS Algorithm

All parts in this section are ultimately combined to represent the proposed PFIS algorithm shown below:

; PFIS algorithm

; Input: Current CGF Situations, Predicted CGF Situations, Predicted Enemy Target Situations

; Output: Best tactics number in Table I

1. Build fuzzy knowledge base (FKB).
2. Generate the control alternatives, which are composed of CGF's decision space.
3. Calculate performances caused by the control alternatives through fuzzification interface with FKB.
4. Choose the best tactics number in Table I through FIE using IF-THEN rules for reasoning.

IV. Simulation Experiments

This paper verifies the performance of IMDS using PFIS algorithm with two types of fighter flying data used as the enemy target's flying trajectory. Before simulation, some parameters must be set up. The time constants τ_x and τ_z for dynamic delay model of control variables n_x and n_z are set to 0.1. In the dynamic delay model of rolling angle ϕ, the natural frequency ω_n and damping ratio ξ are set to be 10 and 0.7 respectively. The parameters of PFIS are set up as follows. In the relative distance membership function, CGF's best shooting distance R_m is set to be 609.59 meters and the standard deviation σ is set to be 304.79 meters. In the velocity membership function, the maximum velocity of advanced fighter V_{max} is set to be 306 meters per second (0.9 Mach). In the height membership function, CGF's minimum flight height h_o is set to be 1523.99 meters. The sample period T is set to be 0.01 second. The time delay parameter n for CGF's flight dynamic equations is set to be 3.

This paper uses Matlab as the simulation environment, and verifies the performance of proposed algorithm using two different kinds of enemy target's flying trajectories, includes non-maneuvering, maneuvering capabilities. In this paper, the development of IMDS is based on the assumption that CGF can produce an optimal strategy based on its abilities of accurately predicting the future positions of its enemy target. In this section, the main priority of the simulations is to produce results proving that IMDS could effectively choose an optimal flight tactic. Also, to see whether giving the predicted step number l a different value would effect the decision making of IMDS, as a method to validate the robustness of this system. In order to analyze whether the performance of the IMDS would be hindered with two different predicted step numbers l=1 (without capability of predicting the enemy target for CGF) and l=100 (with capability of predicting the enemy target for CGF). In addition, a different predicted step number l can be regarded as the ability of the CGF to predict enemy flight patterns.

A. Enemy Target with Trajectory non-maneuvering capabilities

In this case, the CGF's three-dimensional initial position is set as 3047.99 meters, 0 meters and 1523.99 meters respectively. Its initial velocity is 204 meters per second (0.6 Mach). The initial path angle and heading angle are set to be 0 radians (0 degrees) and 0 radians (0 degrees). The enemy target's three-dimensional initial position is set to be 3047.99 meters, 3047.99 meters and 1523.99 meters respectively. Its initial velocity is 204 meters per second (0.6 Mach). The initial path angle and heading angle are set to be 0.52 radians (30 degrees) and 2.51 radians (144 degrees) respectively.

1) Without predicted trajectory

When the predicted step number l is set to be 1 (without capability of predicting the enemy target for CGF), simulation results are shown as Fig. 10 and Fig. 11.

The changes in the trajectory of the CGF and the Enemy Target in a 3D environment are shown in Fig. 10. The figure shows the enemy target at 1524 meters above the ground, spaced 3048 meters, apart from the CGF, flying at a 144 degree angle (heading southeast), climbing at a 30 degree angle, flying at a speed of 0.6 Mach, escaping from the CGF. The figure also shows the CGF at 1524 meters off the ground, facing in a 0 degree angle (heading directly north), and flying at a speed of 0.6 Mach, in pursuit of the enemy target. The decision making process of the IMDS can allow the CGF to speed up in linear travel, make a right turn to intercept the enemy, and in 20 seconds, reach optimal air combat requirements.

© 2008 ACADEMY PUBLISHER

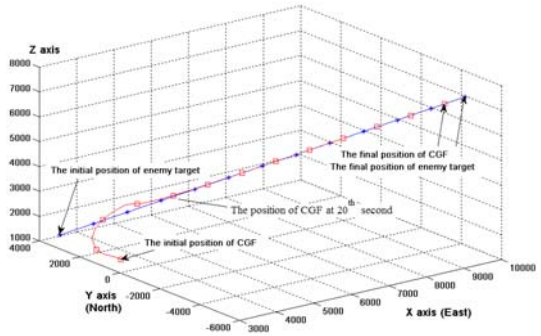

Figure 10. Three-dimensional trajectories of CGF and enemy target with the predicted step number *l* is 1

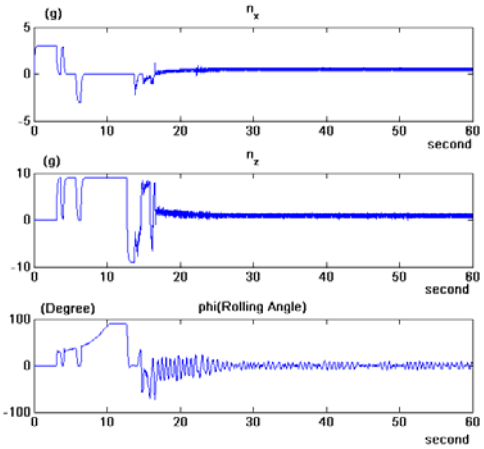

Figure 11. The variation of three control variable of CGF with the predicted step number *l* is 1

Fig. 11, composed of three graphs, represents the different aspects of CGF's three control variables. The upper row of graph is the first control variable; n_x represents the load factor along the direction of V (with graph axes in g's and seconds), which can be translated into the thrust force with units in g's. The g in this case can be ranged from 0 g to ±3 g's. A positive g value represents increased throttle and acceleration, a negative g value represents decreased throttle and deceleration. The delay time it takes for 0 g to reach ±3 g's is 0.1 second. The middle row of graph is the second control variable n_z, which is the load factor of the line perpendicular to the flight velocity direction of CGF, which can be transformed into the pitch force. Its units are also in g's. The values can range from 0 g to ±9 g. The delay time it take for n_z to reach ±9 g from 0 g is 0.1 seconds. If n_z >0, the CGF is performing a left or right turn, or an upward climb, and if n_z <0, CGF is performing a downward decent. The bottom row of graph is the third control variable, which is the rolling angle ϕ. The rolling angle can be transformed into the rolling force, with its axes units in degrees and seconds. When ϕ >0, the CGF is performing a roll to the right, when ϕ <0, the CGF is performing a roll to the left. The delay time for ϕ to reach ±90 degrees from 0 degrees is 1 second.

2) With predicted trajectory

When the predicted step number is set to be 100 (CGF can predict the position of the enemy target for 1 second), simulation results are shown as Fig. 12 and Fig. 13.

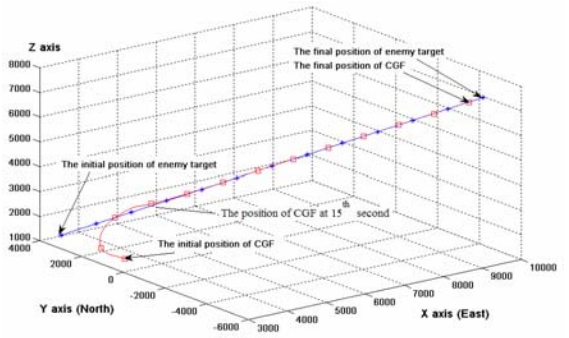

Figure 12. Three-dimensional trajectories of CGF and enemy target with the predicted step number *l* is 100

The changes in the trajectory of the CGF and the Enemy Target in a 3D environment are shown in Fig. 12. The figure shows the enemy target at 1524 meters above the ground, spaced 3048 meters, apart from the CGF, flying at a 144 degree angle (heading southeast), climbing at a 30 degree angle, flying at a speed of 0.6 Mach, escaping from the CGF. The figure also shows the CGF at 1524 meters off the ground, facing in a 0 degree angle (heading directly north), and flying at a speed of 0.6 Mach, in pursuit of the enemy target. The decision making process of the IMDS can allow the CGF to speed up in linear travel, make a right turn to intercept the enemy, and in 15 seconds, reach optimal air combat requirements.

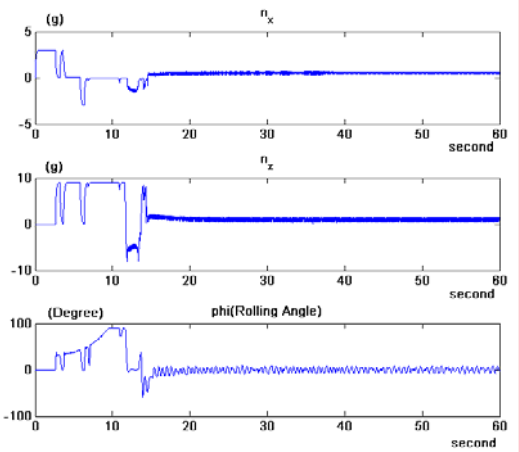

Figure 13. The variation of three control variable of CGF with the predicted step number *l* is 100

Fig. 13, composed of three graphs, represents the different aspects of CGF's three control variables. The meaning of the three graphs is the same as Fig. 11.

3). Performance comparison

By observing Fig. 10, it is found that CGF using IMDS with predicted step number *l* is 1 and enters optimal overall flight status by 20 seconds. In Fig. 12, CGF achieves optimal flight status by 15 seconds with

© 2008 ACADEMY PUBLISHER

predicted step number *l* is 100, and requires a shorter flying distance and chasing time than with predicted step number *l* is 1.

B. Enemy Target with Trajectory maneuvering capabilities

In this case, the CGF's three-dimensional initial position is set as 3047.99 meters, 0 meters and 1523.99 meters respectively. Its initial velocity is 204 meters per second (0.6 Mach). The initial path angle and heading angle are set to be 0 radians (0 degrees) and 0 radians (0 degrees). The enemy target's three-dimensional initial position is set to be 3047.99 meters, 3047.99 meters and 1523.99 meters respectively. Its initial velocity is 204 meters per second (0.6 Mach). The initial path angle and heading angle are set to be 0.52 radians (30 degrees) and 3.14 radians (180 degrees) respectively.

1) Without predicted trajectory

When the predicted step number *l* is set to be 1 (without capability of predicting the enemy target for CGF), simulation results are shown as Fig. 14 and Fig. 15.

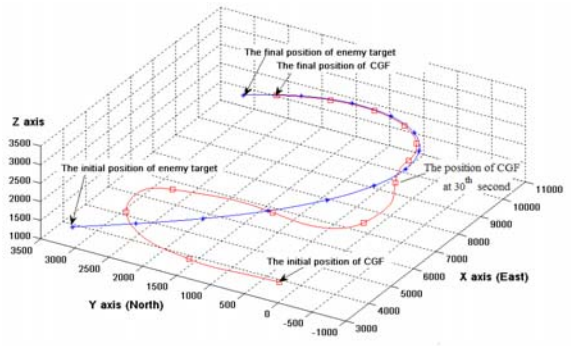

Figure 14. Three-dimensional trajectories of CGF and enemy target with the predicted step number *l* is 1

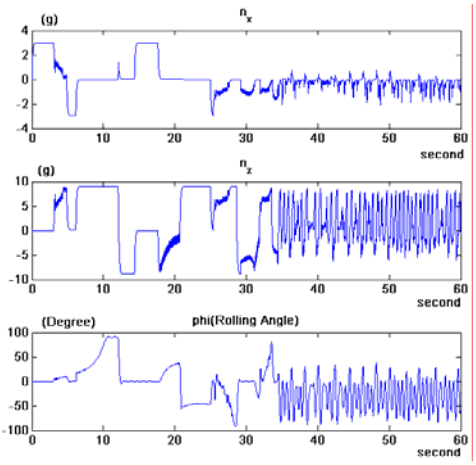

Figure 15. The variation of three control variable of CGF where the predicted step number *l* is 1

The changes in the trajectory of the CGF and the Enemy Target in a 3D environment are shown in Fig. 14. The figure shows the enemy target at 1524 meters above the ground, spaced 3048 meters, apart from the CGF, flying at a 180 degree angle (heading south), climbing at a 30 degree angle, flying at a speed of 0.6 Mach, escaping from the CGF with a heading angle variation rate (1 degree/second). The figure also shows the CGF at 1524 meters off the ground, facing in a 0 degree angle (heading directly north), and flying at a speed of 0.6 Mach, in pursuit of the enemy target. The decision making process of the IMDS can allow the CGF to speed up in linear travel, make a right turn, left turn and right turn to intercept the enemy, and in 30 seconds, reach optimal air combat requirements.

Fig. 15, composed of three graphs, represents the different aspects of CGF's three control variables. The meaning of the three graphs is the same as Fig. 11.

2) With predicted trajectory

When the predicted step number *l* is to be 100 (CGF can predict the position of the enemy target for 1 second), simulation results are shown as Fig. 16 and Fig. 17.

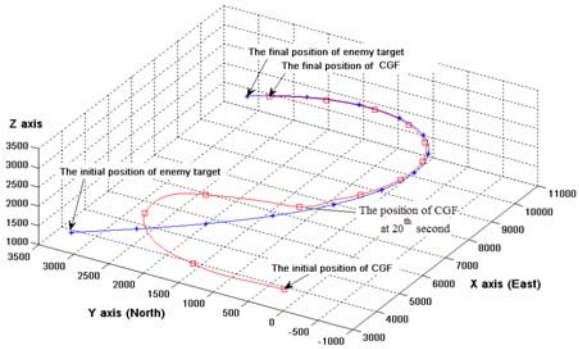

Figure 16. Three-dimensional trajectories of CGF and enemy target with the predicted step number *l* is 100

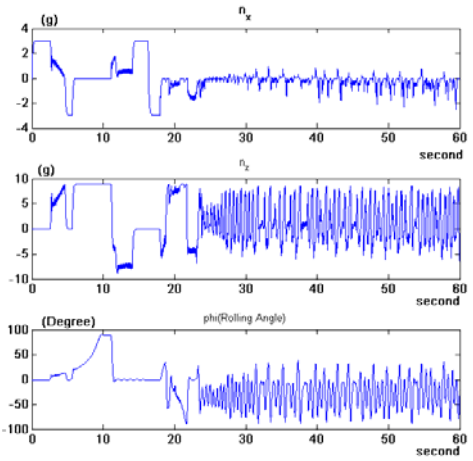

Figure 17. The variation of three control variable of CGF where the predicted step number *l* is 100

The changes in the trajectory of the CGF and the Enemy Target in a 3D environment are shown in Fig. 16. The figure shows the enemy target at 1524 meters above the ground, spaced 3048 meters, apart from the CGF, flying at a 180 degree angle (heading south), climbing at

© 2008 ACADEMY PUBLISHER

a 30 degree angle, flying at a speed of 0.6 Mach, escaping from the CGF with a heading angle variation rate (1 degree/second). The figure also shows the CGF at 1524 meters off the ground, facing in a 0 degree angle (heading directly north), and flying at a speed of 0.6 Mach, in pursuit of the enemy target. The decision making process of the IMDS can allow the CGF to speed up in linear travel, make a right turn, left turn and right turn to intercept the enemy, and in 20 seconds, reach optimal air combat requirements.

Fig. 17, composed of three graphs, represents the different aspects of CGF's three control variables. The meaning of the three graphs is the same as Fig. 11.

3). Performance comparison

By observing Fig. 14, it is found that CGF using IMDS with predicted step number *l* is 1 and enters optimal overall flight status by 30 seconds. In Fig. 16, CGF achieves optimal flight status by 20 seconds with predicted step number *l* is 100, and requires a shorter flying distance and chasing time than with predicted step number *l* is 1.

V. Discussion

This section will discuss on the relationship between the performance for CGF and the predicted step number *l*. As Fig. 18, by observing the membership function value, μ, comparison for enemy target with trajectory maneuvering capabilities, it is found that the optimal status chasing time of CGF with prediction capability for enemy target is faster than without prediction capability, while the maximum value of μ is lower in the stable tracing situation.

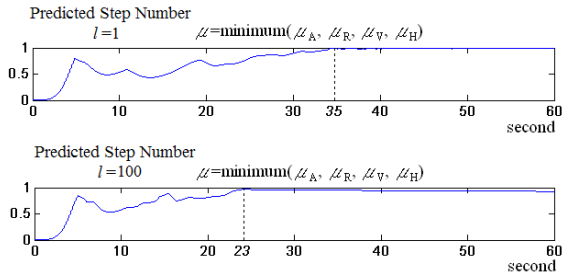

Figure 18. Performance comparison between predicted step number is 1 (without prediction capability for enemy target) and predicted step number is 100 (with prediction capability for enemy target).

The chasing time for CGF achieving the optimal flight status with respect to predicted step number *l* is shown as Fig. 19. In Fig. 19, the chasing time can be fast effectively by increasing the predicted step number *l*.

The meaning of CGF's optimal flight status is that its μ achieves the maximum value for all tracing period. The maximum value of μ with respect to predicted step number *l* is shown as Fig. 20. By observing Fig. 19 and Fig. 20, the chasing time for achieving the CGF's optimal status can be fast with increasing *l*, while the maximum value of μ can be decreasing.

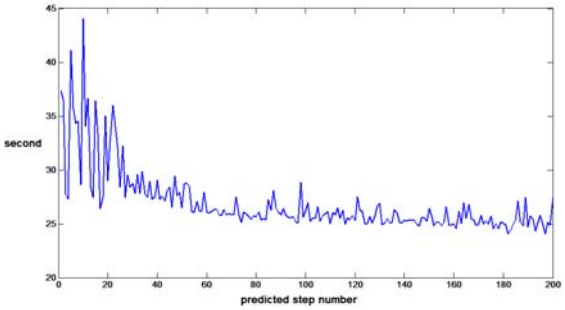

Figure 19. The chasing time for CGF achieving the optimal flight status with respect to predicted step number *l*.

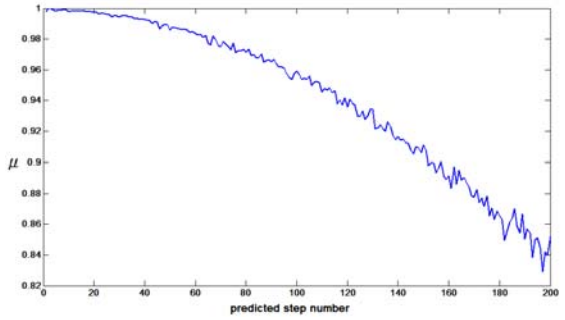

Figure 20. The maximum value of μ with respect to predicted step number *l*.

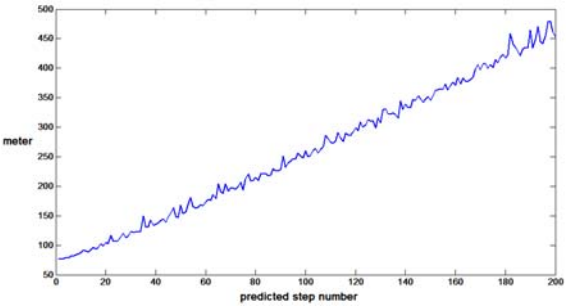

Figure 21. The 3-dimensional position error between the CGF and the tracing targeted point at 60th second with respect to *l*.

Fig. 21 shows the 3-dimensional position error between the CGF and the tracing targeted point at 60th second with respect to *l*. The tracing targeted point is the position of the optimal attacking distance behind the enemy target. By observing Fig. 21, it is found that the position error increases along with the predicted step number *l* increases. Fig. 22 shows the comparison results of 3 different predicted step number *l* and the trajectories are mapped out on the X-Y plane. In Fig. 22, the flight path length decreases along with predicted step number *l* increases.

The results of this section show that the predicted step number *l* will affect the performances of CGF. The predicted step number *l* increases, some performance of CGF increases, such as the 3-dimensional position error between the CGF and the tracing targeted point at 60th second with respect to *l*, which is shown as Fig. 22. The chasing time for CGF achieving the optimal flight status and the maximum value of μ decrease along with the predicted step number *l* increases.

© 2008 ACADEMY PUBLISHER

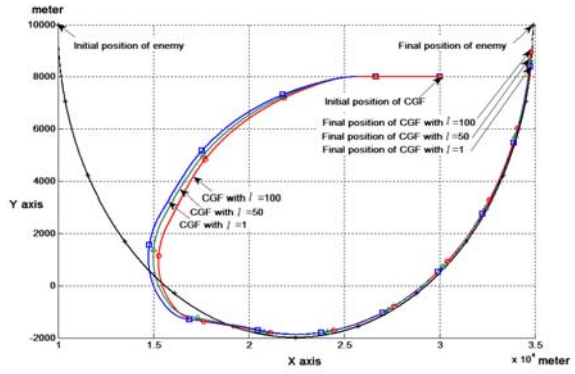

Figure 22. The flight path comparison results of 3 different predicted step number *l* and the trajectories are mapped out on the X-Y plane.

VI. CONCLUSION

In this paper, we propose PFIS algorithm to generate best control command for CGF in an air combat environment. This paper uses PFIS as intelligent maneuvering decision system which incorporates human thinking abilities. The proposed method was then verified with a set of fighter flying data used as the enemy target's flying trajectory. The simulation results show that PFIS can enable CGF to achieve the best status over the enemy target. In the discussion section, the results show that the predicted step number *l* will affect the performances of CGF. In future works, we will put effort in discussing methods in more complex air combat environments.

REFERENCES

[1] M. Edwards, E. Jr. Santos, S. B. Banks, and M. R. Stytz, "Computer generated intelligent companions for distributed virtual environments," in *Proc. IEEE Conf. Tools with Artificial Intelligence*, Toulouse, France, pp. 450-452, Nov. 1996.

[2] S. B. Banks, E. Jr. Santos, and M. R. Stytz, "Enhancing behavioral fidelity within distributed virtual environments," in *Proc. IEEE Conf. Tools with Artificial Intelligence*, Newport Beach, CA, USA, pp. 514-521, Nov. 1997.

[3] H. Akimoto, K. Ono, K. Kayama, K. Kawano, and M. Yoshida, "Consideration to computer generated force for defence systems," in *Proc. IEEE Conf. Computational Intelligence and Multimedia Applications*, Yokusika, Japan, pp. 205-209, Oct 30-Nov. 1, 2001.

[4] M. Brandolini, A. Rocca, A. G. Bruzzone, C. Briano, and P. Petrova, "Poly-functional intelligent agents for computer generated forces," in *Proc. IEEE Conf. Simulation*, Washington, D.C., USA, pp. 514-521, Dec. 2004.

[5] M. Y. Fei and G. G. Hong, "A Modeling and Simulation Framework for Computer Generate Force," in *Proc. IEEE Conf. Smart Manufacturing Application*, Korea, pp. 90-94, Apr. 2008.

[6] X. Y. Yang, G. H. Gong and Y. Tian, "Optimal Game Theory in Complicated Virtual-modeling and CGF Decision-making with Multi-granularities," in *Proc. IEEE Conf. Smart Manufacturing Application*, Korea, pp. 95-99, Apr. 2008.

[7] R. Issacs, *Differential Games*. Kreiger, Huntigton, NY, 1965.

[8] P. K. A. Menon and E.L. Duke, "Time-optimal aircraft pursuit evasion with a weapon envelope constraint," *J. Guid. Control Dyn.*, vol. 15, no. 2, pp. 448-456, 1992.

[9] K. Virtanen, T. Raivio, and R. P. Hamalainen, "Modeling pilot's sequential maneuvering decisions by multistage influence diagram," *J. Guid. Control Dyn.*, vol. 27, no. 4, pp. 665-677, 2004.

[10] B. S. Chen, C.S. Tseng, and H. J. Uang, "Fuzzy differential games for nonlinear stochastic systems: suboptimal approach," *IEEE Trans. Fuzzy Syst.*, vol. 10, no. 2, pp. 222-233, April 2002.

[11] K. H. Hsia and J. G. Hsieh, "A first approach to fuzzy differential game problem: Guarding a territory," *Fuzzy Sets Syst.*, vol. 55, no. 2, pp. 157-167, April 1993.

[12] Y. S. Lee, K. H. Hsia, and J. G. Hsieh, "A strategy for a payoff-switching differential game based on fuzzy reasoning," *Fuzzy Sets Syst.*, vol. 130, no. 2, pp. 237-251, Sep. 2002.

[13] T. Y. Sun, S. J. Tsai, Y. N. Lee, S. M. Yang and S. H. Ting, "The Study on Intelligent Advanced Fighter Air Combat Decision Support System," in *Proc. IEEE Conf. Information Reuse and Integration*, Hawaii, USA, pp. 39-44, Sep. 2006.

Tsung-Ying Sun was born in Hualien, Taiwan, in 1954. He received his B.Sc. in Industrial Education from the National Kaohsiung Normal University, Kaohsiung, Taiwan, in 1976, and received M.Sc. and Ph.D. degrees in electrical engineering from National Taiwan University of Science and Technology, Taipei, Taiwan, in 1992 and 2001, respectively.

He has been the Director of National Hualien Industrial Vocational Senior High School, Hualien, Taiwan, R.O.C. for seven years. He is currently an Associate Professor in the Department of Electrical Engineering, National Dong Hwa University, Hualien, Taiwan, R.O.C. His research interests include computational intelligence, intelligent signal processing, intelligent transportation system, and embedded DSP-based system co-design.

Shang-Jeng Tsai received the B.S. and M.S. degrees in electrical engineering from National Taiwan Ocean University, Keelung and National Dong Hwa University, Hualien, Taiwan, R.O.C., in 2000 and 2002, respectively.

He is currently a doctorate candidate in the department of electrical engineering of National Dong Hwa University, Hualien, Taiwan, R.O.C. His research interests are in computational intelligence and nonlinear dynamical control system theories.

Chih-Li Huo received the B.S. degrees in electrical engineering from I-Shou University, Kaohsiung, Taiwan, R.O.C., in 2007.

He is currently a master degree student in the department of electrical engineering of National Dong Hwa University, Hualien, Taiwan, R.O.C. His research interests are in computational intelligence and nonlinear dynamical control system theories, and their applications to intelligent transportation systems and intelligent computer generated forces decision making system.

© 2008 ACADEMY PUBLISHER